Article

Random Poly(Amino Acid)s Synthesized by Ring Opening Polymerization as Additives in the Biomimetic Mineralization of CaCO₃

**Vladimir Dmitrovic [1], Gijs J.M. Habraken [2], Marco M.R.M. Hendrix [1],
Wouter J.E.M. Habraken [1,3], Andreas Heise [2,4], Gijsbertus de With [1]
and Nico A.J.M Sommerdijk [1,***

[1] Laboratory of Materials and Interface Chemistry and Soft Matter CryoTEM Unit,
    Department of Chemical Engineering and Chemistry, Eindhoven University of Technology,
    P.O. Box 513, Eindhoven 5600 MB, The Netherlands; E-Mails: v.dmitrovic@tue.nl (V.D.);
    m.m.r.m.hendrix@tue.nl (M.H.); g.d.with@tue.nl (G.W.);

[2] Laboratory of Polymer Chemistry, Eindhoven University of Technology, P.O. Box 513,
    Eindhoven 5600 MB, The Netherland; E-Mail: gijs.habraken@gmail.com (G.H.)

[3] Max Planck Institute of Colloids and Interfaces, Research Campus Golm, Am Mühlenberg 1,
    D-14424 Potsdam, Germany; E-Mail: Wouter.Habraken@mpikg.mpg.de

[4] School of Chemical Sciences, Dublin City University, Glasnevin, Dublin 9, Ireland;
    E-Mail: andreas.heise@dcu.ie

* Author to whom correspondence should be addressed; E-Mail: n.sommerdijk@tue.nl;
  Tel.: +31-402-475-870; Fax: +31-402-445-619.

Abstract: Biominerals such as bones, teeth and seashells, very often have advanced material properties and are a source of inspiration for material chemists. As in biological systems acidic proteins play an important role in regulating the formation of CaCO₃ biominerals, we employ poly(amino acid)s to mimic the processes involved in the laboratory. Here we report on the synthesis of random aminoacid copolymers of glutamic acid (Glu), lysine (Lys) and alanine (Ala) using the ring opening polymerization (ROP) of their respective *N*-carboxy anhydrides (NCA). The synthetic approach yields a series of polymers with different monomer composition but with similar degrees of polymerization (DP 45–56) and comparable polydispersities (PDI 1.2–1.6). Using random copolymers we can investigate the influence of composition on the activity of the polymers without having

to take into account the effects of secondary structure or specific sequences. We show that variation of the Glu content of the polymer chains affects the nucleation and thereby also the particle size. Moreover, it is shown that the polymers with the highest Glu content affect the kinetics of mineral formation such that the first precipitate is more soluble than in the case of the control.

Keywords: biomineralization; polypeptide; NCA; vaterite; hybrid materials

1. Introduction

Biological organisms employ inorganic minerals and biocomposites with complex structures to fulfill biological functions including skeletal support and protection of soft tissue [1–4]. It is well recognized that acidic proteins existing in these mineralized tissues fulfill some important functions in controlling mineral formation, including the control over nucleation, growth and polymorph selection [5–8]. This has been documented most extensively for calcium carbonate, the most abundant crystalline biomineral. Biogenic calcium carbonate exists in several polymorphic forms of which calcite and aragonite are the most common ones, but also the metastable forms vaterite and amorphous calcium carbonate (ACC) are observed.

Several acidic proteins have been demonstrated to interact with growing calcium carbonate crystals *in vitro*, not only changing polymorphism, but also leading to modifications in the shape of the crystals [9,10] as well as to their occlusion within the crystalline matrix [11,12]. This is of immediate importance for the mechanical properties of these materials: Where single crystals of synthetic calcite cleave easily along the (10•4) planes, most biogenic calcite is much more resistant to fracture due to the presence of the acidic proteins occluded within the crystals [13,14]. Acidic macromolecules are therefore considered to play a key role in biomineralization processes [15–17]. Nevertheless, there are other characteristics of proteins which play important roles in biomineralization such as the total net charge of the chain, hydrophobicity and hydrogen bonding capacity [18]. To date however, despite many years of research, little information is available about the structure-activity relationships in the proteins that control the formation of calcium carbonate in nature.

Already for decades poly(amino acid)s and their copolymers (generally referred to as synthetic copolypeptides) have attracted interest as models for natural polypeptides and proteins [19–21]. A convenient way to prepare these amino acid based polymers is the ring-opening polymerization of amino acid *N*-carboxyanhydrides (NCAs) [22–24]. Recently, the increased demand for biodegradable and biocompatible polymers has renewed the interest in this class of polymers and thus, the chemistry of amino acid NCAs. With the development of new approaches towards controlled NCA polymerization, it has become possible to synthesize high molecular weight polypeptides with control over polydispersity index (PDI) and polymer architecture [25–36].

In our previous work [37], we demonstrated ring opening polymerization as a powerful tool to synthesize poly(amino acid)s with random composition and without secondary structure (we use the term "polyamino acids" to emphasize the random polymer character of these macromolecules and to differentiate them from peptides with a specific sequence). We investigated the influence of negative

charge and hydrophobicity in copolymers of aspartic acid (Asp), glutamic acid (Glu) and alanine (Ala) on $CaCO_3$ crystallization. It was demonstrated that the Glu/Asp/Ala ratio has a significant influence on the crystal morphology. Furthermore, by fluorescent labeling of the poly(amino acid)s their inclusion in the final product could be demonstrated. Here we show that ROP is a convenient technique to synthesize sets of random poly(amino acid)s with a composition tuned to their function. The poly(amino acid)s presented here were synthesized with different mol percentages of Glu (negatively charged), Lys (positively charged) and Ala (hydrophobic) in the chains. Furthermore, we used a limited set of these polymers with increasing relative amounts of Glu in the chain to address the influence of negative charge and the amount of acidic residues within a chain on the crystallization of $CaCO_3$. Depending on the monomer composition of the polymers we found that they can inhibit nucleation, change polymorph selection as well as the size and morphology of the crystals. We discuss the composition-activity relations and assign specific changes in nucleation of crystals to the amino acid composition and therefore to the physicochemical characteristics of the poly(amino acid)s.

2. Experimental Section

2.1. Materials

Triphosgene, α-pinene, benzylamine, trifluoroacetic acid (TFA), HBr/acetic acid, *N*-dicyclohexylcarbodiimide, *N*-hydroxysuccinimide and deuterated TFA were purchased from Sigma-Aldrich (USA). L-Alanine, γ-benzyl-L-glutamate, and N_ε-benzylcarbonyl-L-lysine were purchased from Bachem (Switzerland). DMF, THF, ethylacetate, n-heptane and diethylether were ordered from Biosolve. For the titration experiments, NaOH Pellets (≥ 98%, anhydrous, Sigma S8045), HCl 25% (Merck 100316), Calcium Chloride Dihydrate (≥ 98%, Sigma-Aldrich 22350-6) sodium carbonate (anhydrous, Merck 106392), sodium bicarbonate (GR for analysis, Merck 106329) were applied.

2.2. Synthesis

2.2.1. Synthesis of *N*-Carboxyanhydride (NCA) of γ-Benzyl-L-glutamate

In a round bottom flask γ-benzyl-L-glutamate (15 g, 63 mmol), α-pinene (25.6 g, 187 mmol) and ethyl acetate (120 mL) were added and stirred under reflux for 30 min at 90 °C in an oil bath. In a separate beaker triphosgene (9.36 g, 30 mmol) was dissolved in 60 mL of ethyl acetate. After 30 min the triphosgene solution was slowly added to the glutamic acid solution (one drop per second). When all the triphosgene solution was added and there was no solid glutamic acid remaining at the bottom of the flask, the reaction was stopped (approx. 3h). By using rotary evaporation the volume of the solution was reduced to approximately 30%. The polymer was precipitated by dropping in n-heptane (120 mL). After recrystallization from the mother liquor, white crystals of glutamic acid were obtained. Yield: 13.7 g; 57.9 mmol; 84 mol%. ^{1}H-NMR (400MHz, $CDCl_3$, δ, ppm): 2.20 (m, 2H, CH_2), 2.59 (t, 2H, CH_2, j = 6.8 Hz), 4.37 (t, H, CH_2O, J = 6.1 Hz), 5.14 (s, 2H, CH_2O), 6.57 (s, 1H, NH), 7.36 (m, 5H, ArH).

2.2.2. Synthesis of *N*-Carboxyanhydride (NCA) of N_ε-Benzylcarbonyl-L-lysine

In a round bottom flask N_ε-benzylcarbonyl-L-lysine (10 g, 26.6 mmol), α-pinene (11 g, 81 mmol) and ethyl acetate (80 mL) were added and stirred under reflux for 30 min at 90 °C in an oil bath. In a separate beaker triphosgene (6.4 g, 22 mmol) was dissolved in 40 mL of ethyl acetate. After 30 min the triphosgene solution was added to the lysine solution (one drop per second). Further steps were done using the procedure described for γ-benzyl-L-glutamate. Yield: 9.4 g; 33.5 mmol; 86 mol%. ^{1}H-NMR (400MHz, CDCl$_3$, δ, ppm): 1.54 (m, 4H, CH$_2$CH$_2$), 1.90 (m, 2H, CH$_2$), 3.20 (q, 2H, CH$_2$, J = 6.4 Hz), 4.25 (t, 1H, CH, J = 5.1 Hz), 4.90 (s, 1H, NH), 5.10 (s, 2H, CH$_2$O), 7.05 (s, 1H, NH), 7.36 (m, 5H, ArH).

2.2.3. Synthesis of *N*-carboxyanhydride (NCA) of L-alanine

In a round bottom flask ground L-Alanine (6 g, 67 mmol), α-pinene (35 g, 257mmol) and ethyl acetate (250mL) were added and stirred under reflux for 30 min at 90 °C in an oil bath. In a separate beaker triphosgene (38 g, 128 mmol) was dissolved in 100 mL of ethyl acetate. After 30 min the triphosgene solution was added to the alanine solution (one drop per second). Further steps were done using the procedure described for γ-benzyl-L-glutamate. Yield: 5.1 g; 42.96 mmol; 63 mol%. ^{1}H-NMR (400MHz, CDCl$_3$, δ, ppm): 1.57 (d, 3H, CH$_3$, J = 7.0 Hz), 4.46 (q, 1H, C, J = 7.0 Hz), 6.0 (s, 1H, NH).

2.2.4. Random NCA Copolymerization

Polymerization reactions were done in a Schlenk tube under argon flow at 0 °C. The NCA monomers of γ-benzyl-L-glutamate (1.2 g 4.5 mmol), N_ε-benzylcarbonyl-L-lysine (0.7 g, 2.3 mmol) and L-alanine (0.3 g, 2.4 mmol) were added in the Schlenk tube and dissolved in 21 mL of *N,N*-dimethylformamide. After all NCAs were dissolved benzylamine (20 mg, in 1 mL DMF) was added from the stock solution to activate the reaction. The reaction was stirred for four days and then quenched by precipitating the reaction mixture in 200 mL of diethyl ether. After reprecipitation by diethyl ether a white powder was filtered and dried overnight in a vacuum oven at 30 °C. The quantities given above are used for the synthesis of the $E_{16}K_{17}A_{13}$. Quantities for the other poly(amino acid)s were calculated corresponding to the desired polymer composition.

2.2.5. Deprotection of Polyamino Acids

The protected poly(amino acid) (0.5 g) was dissolved in 9 mL of trifluoroacitic acid. When the polyamino acid was completely dissolved, 33% HBr in acetic acid (7 mL) was added to the solution and the mixture was left to stir for 24 h. After 24 h the solution was precipitated in diethyl ether. The polypeptide was allowed to settle on the bottom and the solution was decanted. Diethylether (200 mL) was added and the mixture was stirred for 10 min, after which the solvent was removed by decantation again. This procedure was performed five times to get a clear diethylether solution. After filtration, residual solvent was removed by drying overnight in a vacuum oven at 30 °C. Yield: 0.27 g; 55 wt%.

2.3. Characterization

2.3.1. Size Exclusion Chromatography (SEC)

Size exclusion chromatography in hexafluoroisopropanol (HFIP) was performed on a system equipped with a Waters 1515 Isocratic HPLC pump, a Waters 2414 refractive index detector (40 °C), a Waters 2707 autosampler, a PSS PFG guard column followed by 2 PFGlinear-XL (7 μm, 8 × 300 mm) columns in series at 40 °C. 1,1,1,3,3,3 Hexafluoro-2-propanol (HFIP, Apollo Scientific Limited) with potassium trifluoro acetate (3 g L^{-1}) was used as eluent at a flow rate of 0.8 mL min^{-1}. The molecular weights were calculated against polymethyl methacrylate standards (Polymer Laboratories, Mp = 580 Da up to Mp = 7.1×10^6 Da).

2.3.2. ^{1}H-NMR

^{1}H-NMR analyses were performed on a Bruker ^{1}H-NMR spectrometer type Mercury 400. For measuring the poly(amino acid)s spectra deuterated TFA was used. The composition of poly(amino acid)s was determined by comparing the peak intensities corresponding to the signals characteristic for L-glutamate (2.80 ppm, 2H), L-lysine (2.15 ppm, 2H) and L-alanine (1.70 ppm, 3H).

2.3.3. Titration Experiments

The Metrohm® commercial titration setup was used in all experiments. The setup contains a computer, which runs the software Tiamo 2.1 that controls two 809 Titrando tritrating units, three 2 mL Dosino dosing units and a magnetic stirrer plate. A double junction micro pH glass electrode (6.0234.100) and a polymer membrane (PVC) calcium ion selective electrode (Ca-ISE, 6.0508.110,) were utilized to measure the pH and concentration of free Ca^{2+} ions in solution, respectively; each connected to one of the Titrando 809 stations. The pH electrode was calibrated daily using Metrohm buffer standards at pH = 4.0 (No. 6.2307.100), pH = 7.0 (No. 6.2307.110) and pH = 9.0 (No. 6.2307.120), while the Ca-ISE was calibrated before each experiment.

All solutions were freshly prepared for each experiment utilizing fresh Milli-Q water (resistivity 18.2 MΩ·cm at 20 °C), degassed overnight with N_2. A sodium hydroxide solution of 10 mM was prepared by dissolving NaOH pellets in water, 10mM hydrochloric acid was prepared by the dilution of HCl 25%. Calcium chloride solutions (50 mM) used for titrations and calibrations were obtained by dissolving calcium chloride dihydrate in CO_2 free water. To achieve the desired pH value a 10 mM carbonate buffer was prepared consisting of a mixture of 10 mM sodium carbonate and 10 mM sodium bicarbonate. Experiments were performed in a 80 mL beaker containing a 25 mL 10 mM sodium carbonate/sodium bicarbonate solution set at pH = 9.75. Fifty millimolar calcium chloride solution set at pH = 9.75 was dosed at a rate of 10 μL/min. In experiments with poly(amino acid)s, 10 mg of poly(amino acid) was dissolved in 100 mL of 50 mM calcium chloride solution before starting the experiment. The pH was kept constant by titrating 10mM sodiumhydroxide/hydrochloric acid solutions and measured by the pH electrode at 20 ± 1 °C in all cases. The stirring rate in all performed experiments was 600RPM. All beakers, electrodes and burette tips were cleaned with 10% acetic acid and rinsed with distilled water after every experiment. To convert measured Ca^{2+} activities into

concentrations for the calculation of the activity coefficients the Davies-extended Debye-Huckel Equation was applied [38].

2.3.4. Scanning Electron Microscopy (SEM)

SEM studies of the $CaCO_3$ crystals were performed on a Quanta 3D FEG (FEI company) with a field emission electron gun as electron source at an acceleration voltage of 10 kV and a current between 10–14 pA. For this, precipitated crystals were centrifuged, washed with acetone and air-dried for a day and then placed on a SEM stub with carbon tape. Subsequently, the samples were sputter-coated with a layer of gold applied using a current of 20 mA for 3 min.

2.3.5. Powder X-ray Diffraction (PXRD)

XRD measurements were performed on a Rigaku Geigerflex powder diffractometer with Bragg-Brentano geometry, using copper radiation at 40 kV and 30 mA and a graphite monochromator on the detector side to eliminate the CuK_β radiation. The samples were prepared in a glass capillary. The XRD scans were measured from 10 till 60 (°) 2-theta with a step size of 0.02 (°) and a dwell time of 25 seconds.

2.3.6. Raman Microscopy

The Raman spectrometer (Dilor Labram) was equipped with a Millennia II doubled Nd:YVO$_4$ laser with an excitation wavelength of 632.81 nm operated at a power of 200 mW, 1800 grooves/mm holographic grating and a 1024×256 pixel CCD camera. Spectra were recorded in the region 50–1500 cm^{-1}. Depth profiles, *i.e.*, spectral intensity as a function of the distance of the sampled spot to the surface, was performed by manually adjusting the distance between sample and objective. A 100x magnification, (Olympus, numerical aperture 0.8) ultra long working distance objective was used. The Labram was equipped with a built-in camera, enabling the visualization of the reflected laser light from the inner side of the glass plate. Focal depth zero was determined by minimizing the spot size of this reflected light.
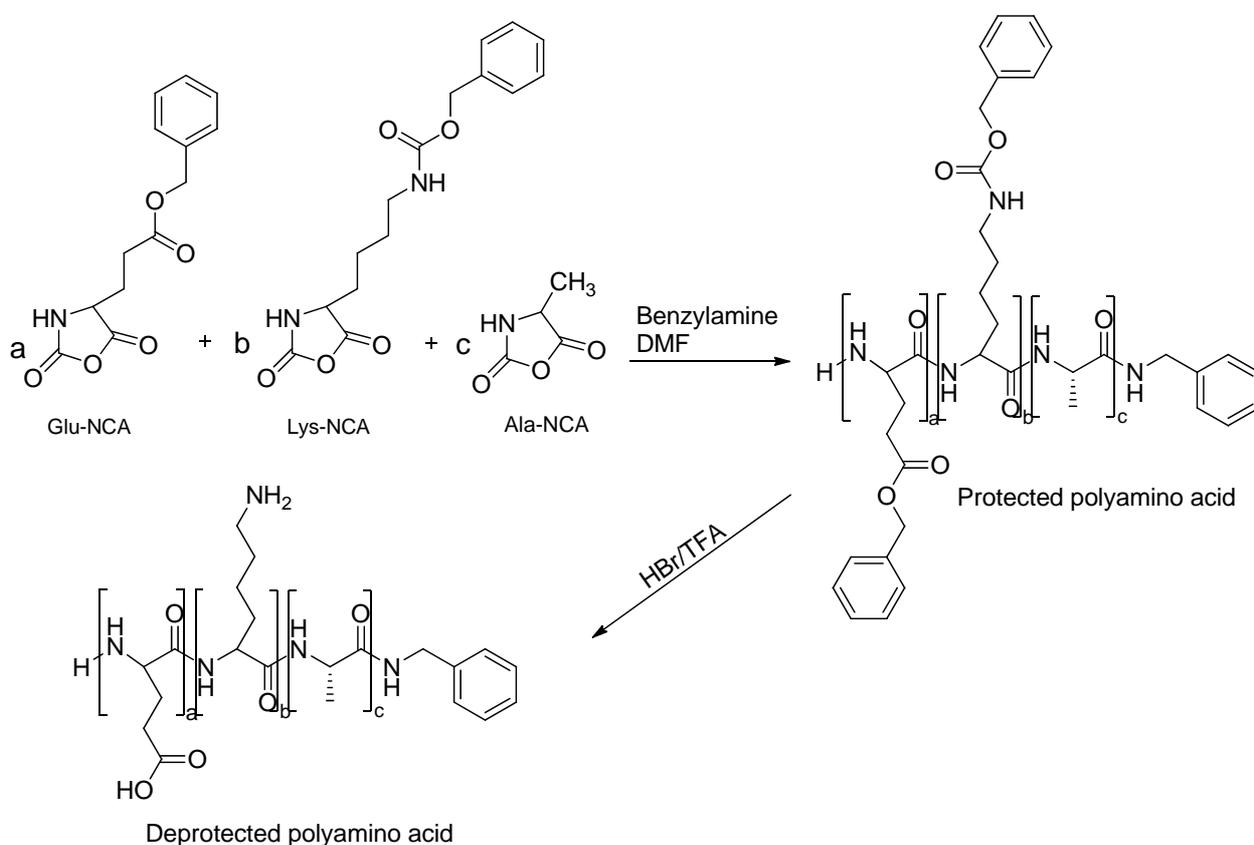
3. Results and discussion

The NCA monomers used were synthesized according to literature procedures by reacting γ-benzyl-L-glutamate, N_ε-benzylcarbonyl-L-lysine or L-alanine with triphosgene using α-pinene as HCl scavenger [39]. During the reaction the initially turbid solutions in all cases became clear, indicating the conversion of the poorly soluble (protected) amino acids into the more soluble NCA monomers. The NCA monomers could be purified by repeated recrystallization from n-heptene and ethylacetate, resulting in white crystals for all monomers.

While the syntheses of **NCA-Glu** and **NCA-Lys** were performed with an acceptable yield (84% and 86%, respectively), for **NCA-Ala** only a low yield was obtained, which was attributed to the low solubility of L-alanine in ethyl acetate. To improve the solubility of L-alanine the crystals were ground to a fine powder, which indeed resulted in an approximately threefold increase of the yield to ~63%. The conversion of L-alanine to **NCA-Ala** was monitored through the evolution of the C=O IR stretch

vibration at 1810 cm^{-1} [40]. FTIR measurements showed that after 6 h of reaction time indeed no further increase in the peak intensity was observed. At this point also the alanine powder at the bottom of the flask had dissolved and the reaction was terminated.

Random co-poly(amino acid)s were prepared by performing the ring opening polymerization of varying amounts of the different NCAs in a Schlenk tube under argon atmosphere using DMF as the solvent and benzylamine as the initiator. The reactions were performed at 0 °C as it was shown previously that this lower temperature avoids side reactions at the chain ends, which commonly lead to in-ring structures and chain-end termination, as well as "in-main-chain" reactions [41,42]. After isolation of the polymers the benzyl protecting groups of the Glu and Lys side chains were removed by dissolution in TFA and by reaction with 33% HBr in acetic acid (Scheme 1).

Scheme 1. NCA polymerization and deprotection of random poly(amino acid)s.

The amount of Glu (E) in the polymers was varied from 33 to 80 mol% while keeping Lys (K) and Ala (A) at equal contributions (33–10 mol%, Table 1). The monomer composition of the polymers was determined from ^{1}H NMR spectra in TFA, integrating characteristic resonances for the different amino acids (Glu 2.80 ppm, 2H; Lys 2.15 ppm, 2H; Ala 1.70 ppm, 3H) using the initiator benzyl group as a standard (Figure 1, Table 1). The degrees of polymerization (DP) and polydispersity index (PDI) were derived from size exclusion chromatography of the protected polymers and NMR analysis of the deprotected ones.

Figure 1. ^{1}H NMR spectra of poly(amino acid) $E_{28}K_9A_7$ before and after deprotection. Arrows indicate characteristic peaks, which were used for the determination of the poly(amino acid) composition. Black (7.50 ppm) initiator benzyl group, blue (2.15 ppm) Lys, red (2.80 ppm) Glu and purple (1.70 ppm) Ala. Deuterated TFA was used as a solvent.
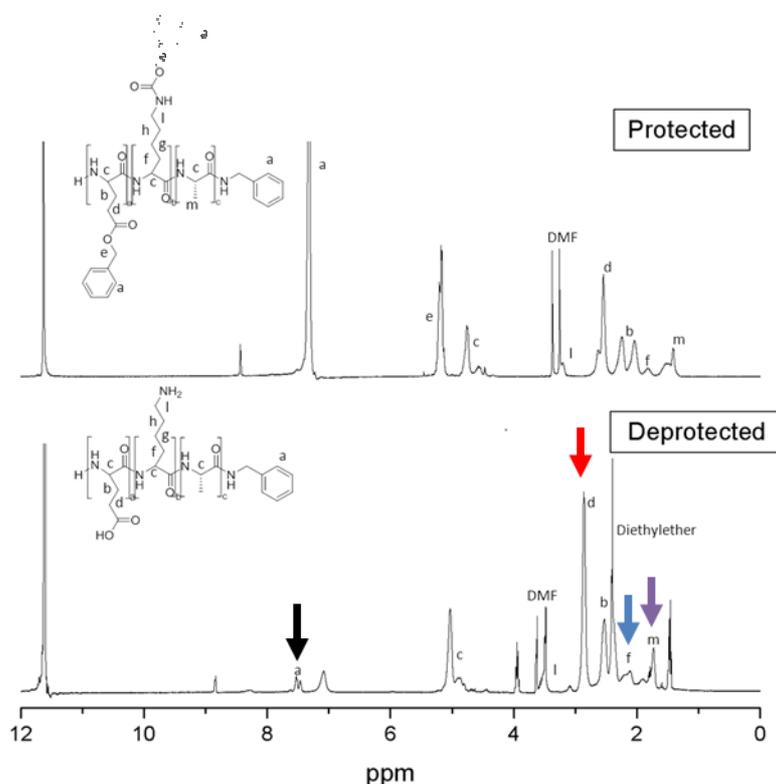

Table 1. Overview of poly(amino acid)s synthesized by NCA amino acid polymerization and data calculated from ^{1}H NMR spectra of deprotected poly(amino acid)s (a) Measured by Size Exclusion Chromatography (SEC) using PMMA standards; (b) Calculated using proton NMR of deprotected poly(amino acid)s.
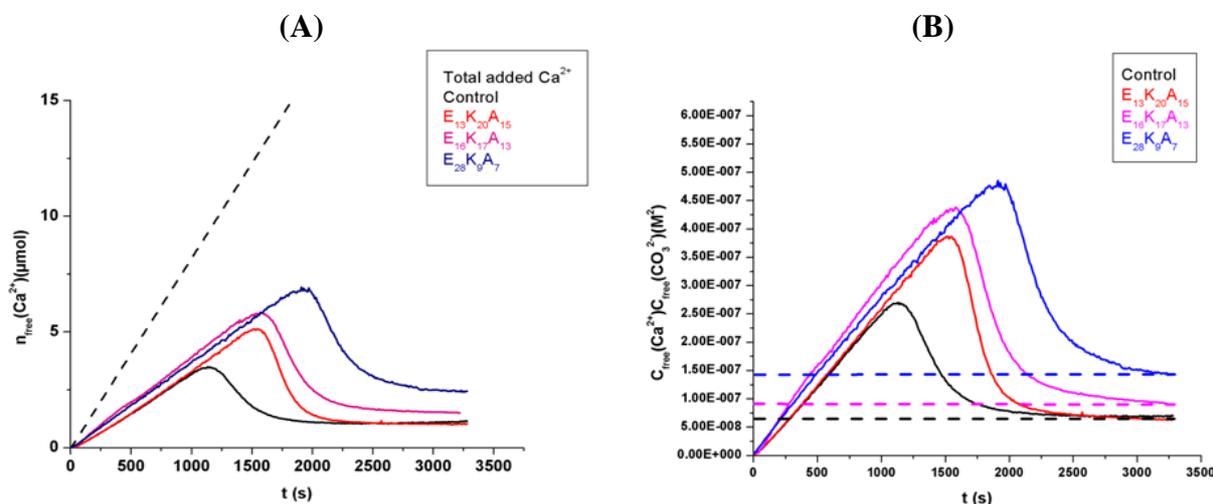
Target composition	DP (a)	Mn (g/mol) (a)	PDI (a)	Experimental composition (b)
$E_{14}K_{14}A_{14}$	56	10400	1.20	$E_{11}K_{25}A_{18}$
$E_{18}K_{12}A_{12}$	50	9600	1.60	$E_{13}K_{20}A_{15}$
$E_{22}K_{10}A_{10}$	50	9700	1.57	$E_{16}K_{17}A_{13}$
$E_{26}K_9A_9$	47	9400	1.45	$E_{21}K_{19}A_{13}$
$E_{34}K_4A_4$	45	9500	1.61	$E_{28}K_9A_7$

Table 1 shows that only a moderate control over DP and PDI was obtained. The DP varied from 45–56 and the PDI between 1.20 and 1.61. Furthermore, it shows that compared to the targeted composition, the incorporation of Glu was less effective leading to the enrichment in Lys and Ala, compared to the targeted composition. Nevertheless a series of polymers with increasing relative Glu content and decreasing Lys and Ala content, which can be used to study the influence of total net charge and hydrophobicity on the nucleation and growth of calcium carbonate, were successfully synthesized.

3.1. Random Poly(Amino Acid)s in CaCO₃ Mineralization

To investigate the influence of the polymer composition on the formation of calcium carbonate, mineralization experiments were performed using three polymers with increasing relative Glu content: $E_{13}K_{20}A_{15}$, $E_{16}K_{17}A_{13}$ and $E_{28}K_9A_7$. The early stages of mineral formation were studied with titration experiments as described by Gebauer *et al.* [43] by titrating a 50 mM CaCl₂ solution (10 µL/min) containing 10 mg of the respective polymers to a 10 mM carbonate buffer (pH = 9.75). During this process the free Ca^{2+} concentration was measured using a calcium ion-selective electrode (Ca-ISE) while the pH of the solution was kept constant by automated addition of 10 mM NaOH solution. It should be noted that in our experiments the polymers are added to the CaCl₂ solution rather than to the carbonate buffer as we observed from similar studies that the calcium ions interact with the polymers. As this interaction changes over time, we choose to equilibrate the polymers in the calcium chloride solution, even though this precludes the possibility to probe the polymer-Ca^{2+} interaction during the titration experiment.

Figure 2. (**A**): Titration experiments showing the development of free calcium concentration in time in the absence of poly(amino acid)s (control, black) and in the presence of $E_{13}K_{20}A_{15}$ (red), $E_{16}K_{17}A_{13}$ (purple) and $E_{28}K_9A_7$ (blue). Dashed line represents total amount of Ca^{2+} titrated in solution; (**B**): Time development of free ion concentration product without poly(amino acid)s (control, black) and in presence of $E_{13}K_{20}A_{15}$ (red), $E_{16}K_{17}A_{13}$ (purple) and $E_{28}K_9A_7$ (blue).

The control reaction (without polymer additives) showed that the measured calcium concentration (the free calcium concentration, $[Ca^{2+}_{free}]$) initially increases proportionally with the amount of calcium added (Figure 2A) but only accounts for approximately 40% of the total calcium concentration ($[Ca^{2+}_{tot}]$). This difference between the added and measured calcium concentrations has been attributed to the formation of nanometer sized pre-nucleation clusters, which were demonstrated to exist in saturated and undersatured solutions in equilibrium with the solute ions. After ~1200 sec a sudden drop in $[Ca^{2+}_{free}]$ is observed marking the nucleation point of the first precipitated phase. After the drop the calcium level stabilizes and the associated free ion concentration product ($[Ca_{free}^{2+}] [CO_3^{2-}]$) can be related to the solubility of the precipitate, which in the work of Gebauer *et al.* was ACC. It was

observed that under different conditions the precipitated ACC had different solubilities, which were related to the crystalline phase that formed from the ACC in a later stage of the reaction. In our experiments only crystalline products were isolated from the reaction medium. As expected under these conditions PXRD and Raman spectroscopy revealed that the mineral phase consisted of vaterite (Figure 3), while SEM analysis revealed the formation of particles with an almond-like morphology and an average size of ~2 μm (Figure 4).

Figure 3. (**A**): X-Ray Diffraction (XRD) data collected from crystals precipitated in the experiment in the presence of $E_{13}K_{20}A_{15}$, $E_{16}K_{17}A_{13}$ and $E_{28}K_9A_7$ clearly proving that these crystals were vaterite. The appearance of a small calcite peak in presence of $E_{28}K_9A_7$ (arrow) is due to the presence of a few calcite crystals in mixture; (**B**): Raman data collected from experiments in the absence of additive (control) and in presence of $E_{13}K_{20}A_{15}$, $E_{16}K_{17}A_{13}$ and $E_{28}K_9A_7$ showing that crystals were vaterite [44]. The peak at around 380 cm^{-1} (red arrow) could be assigned to the glass slide background on which crystals were placed for the measurements.
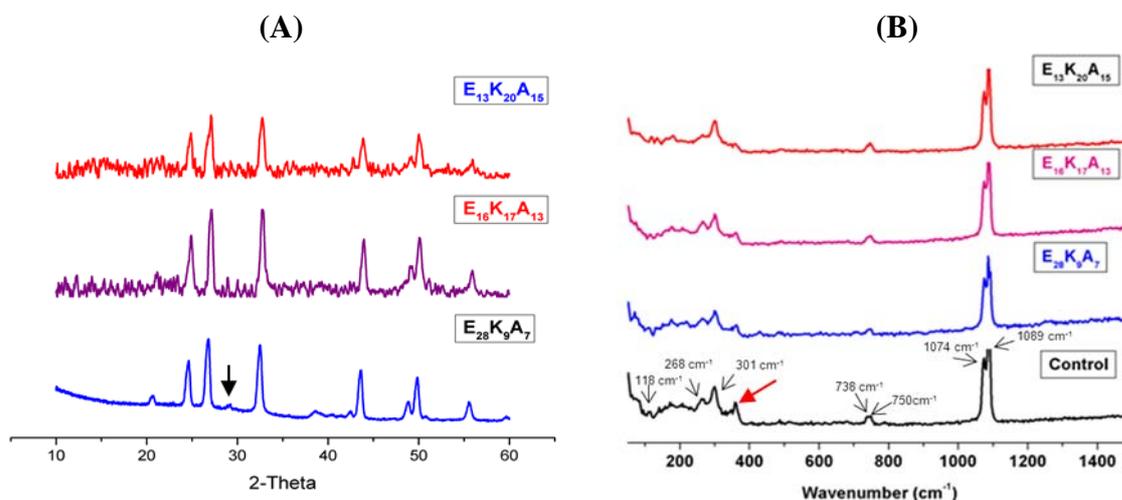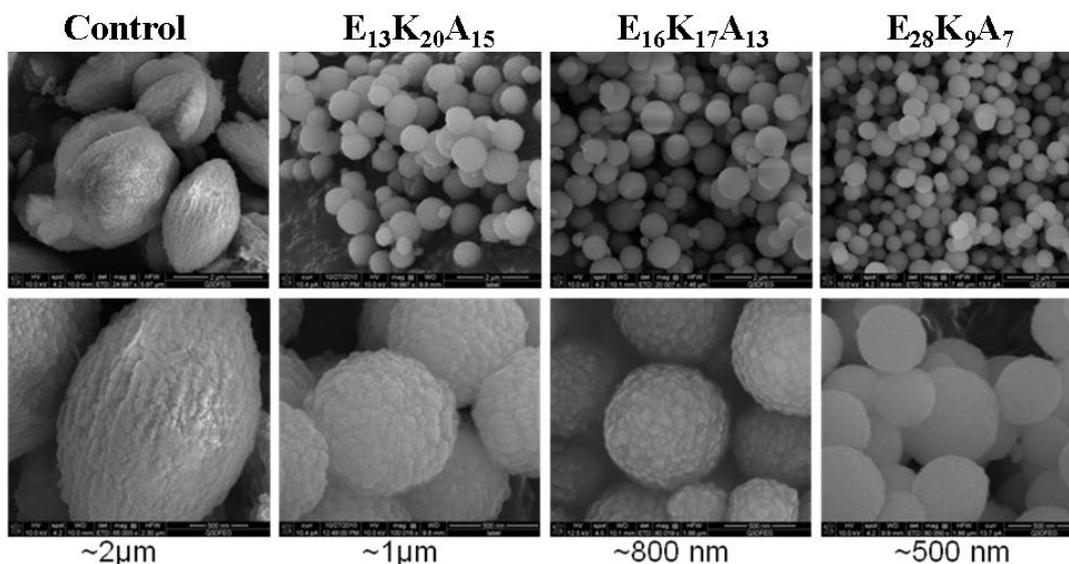

Figure 4. SEM images of particles isolated from solutions.

In contrast to the work of Gebauer *et al.* [43], activity coefficients were used to account for the difference in ionic strength between the Ca^{2+}-Calibration in water (where I = max. 0.003 M) and the titration of Ca^{2+} in an excess of CO_3^{2-} during the reaction (where I $\approx$ 0.014 M, $\gamma_{Ca}^{2+} \approx$ 0.61). The plateau that is observed after nucleation represents an ion concentration product of 7.0×10^{-8} M^2. When the contribution of the activity coefficients is neglected, an ion concentration product of 4.0×10^{-8} M^2 is obtained. This value agrees well with the value of 3.8×10^{-8} M^2 found by Gebauer *et al.* [43].
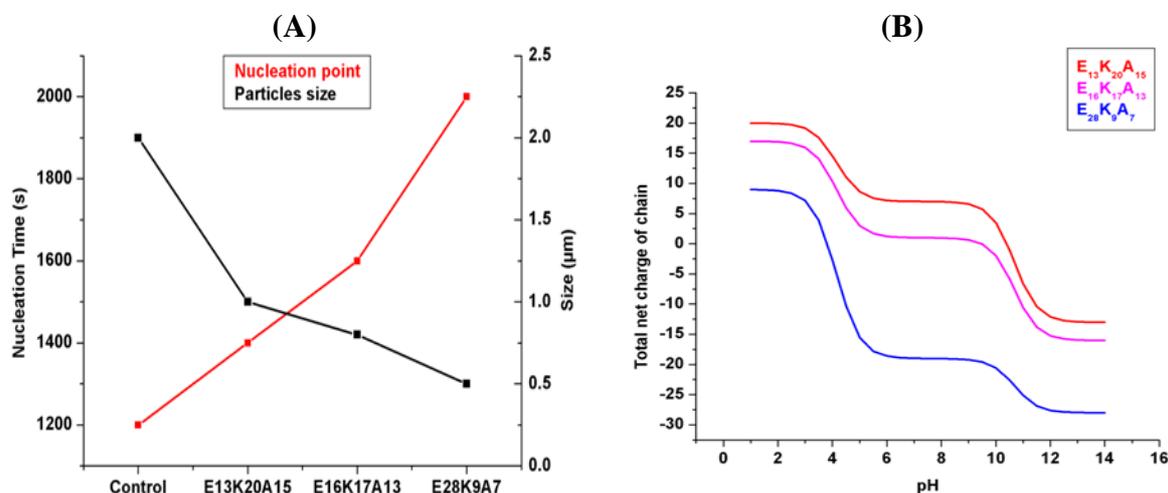
Compared to the control, the presence of polymers leads to the delay in nucleation point for 300, 400 and 800 seconds going from $E_{13}K_{20}A_{15}$, to $E_{16}K_{17}A_{13}$ and $E_{28}K_9A_7$, respectively. The different compositions of the polymers also had a significant effect on the particle size going from ~1.0 μm for $E_{13}K_{20}A_{15}$, to 800 nm for $E_{16}K_{17}A_{13}$ and finally to 500 nm for $E_{28}K_9A_7$ (Figure 4).

The inhibition of nucleation associated with the presence of the polymers (Figure 2) appears to scale with their Glu content. It is well known from the literature that increasing the negative charge in the polymer chain results in the inhibition of $CaCO_3$ nucleation [45,46] and stabilization of a less stable polymorph of $CaCO_3$, *i.e.*, vaterite [47,48]. However, positively charged polymers have also been demonstrated to inhibit the nucleation of calcium carbonate in solution [49]. Hence, one may expect that the net charge of the polymer, rather than the amount of negatively charged monomers, would play a decisive role in the inhibition of nucleation. It can be calculated that at the pH of the experiment (pH 9.75) the total net charge of the polymers is +7 for $E_{13}K_{20}A_{15}$, +1 for $E_{16}K_{17}A_{13}$ and −19 for $E_{28}K_9A_7$. From the observation that the inhibition effect is stronger for $E_{16}K_{17}A_{13}$ (total net charge = +1) than for $E_{13}K_{20}A_{15}$ (total net charge = +7) we therefore must conclude that the effect of the negatively charged Glu is stronger than that of the positively charged Lys and that in fact it is the amount of negatively charged residues that determines the inhibition power of these polymers.

It is well known that the proteins involved in calcium carbonate biomineralization generally are rich in acidic amino acids [50], nevertheless it has recently been emphasized that also positively charged residues may play a significant role [49]. In our previous [37] work, we could see that in similar copolymers containing Asp, Glu and Ala the activity of Asp in modifying calcium carbonate formation is dominant over the activity of Glu. In the present study, we have replaced Asp by Lys in the copolymers. The results obtained show that the activity of the Glu monomers is stronger than that of Lys. Taking into account the respective control experiments we assign the fact that the end products in the current studies are different from our previous study [37] to the different experimental conditions used rather than to a difference in polymer composition. Hence, based on the results from both studies we can speculate that within a (bio)polymer chain, the activity of the above residues (monomers) in modifying calcium carbonate formation follows the order Asp > Glu > Lys.

The observed decrease in particle size from the control to $E_{13}K_{20}A_{15}$, $E_{16}K_{17}A_{13}$ and $E_{28}K_9A_7$ implies an increase in nucleation sites going through this sequence of polymers. This observation can be related to the fact that in the titration experiment the $[Ca^{2+}_{tot}]$ continuously increases and that the inhibiting action of the polymers causes nucleation to occur at a higher supersaturation which is known to lead to decreased particle sizes (Figure 5A).

Figure 5. (**A**): Summary data from titration experiments. Particle size and time at which nucleation occurred without poly(amino acid)s (control) and in the presence of $E_{13}K_{20}A_{15}$, $E_{16}K_{17}A_{13}$, $E_{28}K_9A_7$; (**B**): Calculated total net charge of the same poly(amino acid)s for different pH values.

4. Conclusions

ROP polymerization of NCA monomers under argon flow at 0 °C was used, for the first time, to synthesize random co-poly(amino acid)s composed of Glu, Lys and Ala. The resulting polymers were prepared with different compositions but with comparable degrees of polymerization (DP 45–56) and polydispersities (PDI 1.2–1.6). Three selected poly(amino acid)s with different Glu content were used in a vaterite forming mineralization assay in which calcium ions, containing the poly(amino acid)s, at a constant pH of 9.75 were added to a carbonate buffer. These results showed that increasing the Glu fraction in the polymer chain leads to an increased inhibition of the $CaCO_3$ nucleation and to a decrease in particle size. This effect was attributed to the Glu content rather than to the concomitant variations in the net charge of the poly(amino acid). Interestingly, the poly(amino acid)s with highest Glu content were also able to modify the mineralization process such that the apparent solubility of the precipitated phases increased, as judged by the levels of soluble calcium detected in the solutions after the nucleation.

Overall the ability to synthesize such a set of poly(amino acid)s in which only their composition varies allows us to make direct assessments of the structure activity relationships in biomimetic mineralization experiments. The results presented in this work are part of an on-going project aiming at the use of random amino acid-based copolymers in the biomimetic formation of calcium carbonate based hybrid materials. In the near future we hope to extent the scope of our approach to random co-poly(amino acid)s with four (Glu, Lys Ala, Ser) and five (Glu, Lys Ala, Ser, Asp) different monomers to increase the number of control parameters encrypted in these poly(amino acid)s. With this we aim to eventually understand and control the bioinspired formation of calcium carbonate hybrid materials with advanced material properties.

References

1. Addadi, L.; Joester, D.; Nudelman, F.; Weiner, S. Mollusk shell formation: A source of new concepts for understanding biomineralization processes. *Chem. Eur. J.* **2006**, *12*, 981–987.

2. Addadi, L.; Weiner, S. Control and design principles in biological mineralization. *Angew. Chem. Int. Edit. Engl.* **1992**, *31*, 153–169.

3. Bauerlein, E. Progress in biology, molecular biology, and application. In *Biomineralization*, 2nd ed.; Bauerlein, E., Ed.; WILEY-VCH Verlag GmbH & Co. KGaA: Weinheim, Germany, 2004.

4. Mann, S. *Biomineralization: Principles and Concepts in Bioinorganic Materials Chemistry*; Oxford University Press: Oxford, UK, 2001.

5. Delak, K.; Giocondi, J.; Orme, C.; Evans, J.S. Modulation of crystal growth by the terminal sequences of the prismatic-associated asprich protein. *Cryst. Growth Des.* **2008**, *8*, 4481–4486.

6. Gotliv, B.A.; Addadi, L.; Weiner, S. Mollusk shell acidic proteins: In search of individual functions. *Chem. Biochem.* **2003**, *4*, 522–529.

7. Gotliv, B.A.; Kessler, N.; Sumerel, J.L.; Morse, D.E.; Tuross, N.; Addadi, L.; Weiner, S. Asprich: A novel aspartic acid-rich protein family from the prismatic shell matrix of the bivalve atrina rigida. *Chem. Biochem.* **2005**, *6*, 304–314.

8. Politi, Y.; Mahamid, J.; Goldberg, H.; Weiner, S.; Addadi, L. Asprich mollusk shell protein: *In vitro* experiments aimed at elucidating function in $CaCO_3$ crystallization. *Cryst. Eng. Comm.* **2007**, *9*, 1171–1177.

9. Belcher, A.M.; Wu, X.H.; Christensen, R.J.; Hansma, P.K.; Stucky, G.D.; Morse, D.E. Control of crystal phase switching and orientation by soluble mollusc-shell proteins. *Nature* **1996**, *381*, 56–58.

10. Falini, G.; Albeck, S.; Weiner, S.; Addadi, L. Control of aragonite or calcite polymorphism by mollusk shell macromolecules. *Science* **1996**, *271*, 67–69.

11. Metzler, R.A.; Tribello, G.A.; Parrinello, M.; Gilbert, P.U.P.A. Asprich peptides are occluded in calcite and permanently disorder biomineral crystals. *J. Am. Chem. Soc.* **2010**, *132*, 11585–11591.

12. Metzler, R.A.; Evans, J.S.; Killian, C.E.; Zhou, D.; Churchill, T.H.; Appathurai, N.P.; Coppersmith, S.N.; Gilbert, P.U.P.A. Nacre protein fragment templates lamellar aragonite growth. *J. Am. Chem. Soc.* **2010**, *132*, 6329–6334.

13. Berman, A.; Addadi, L.; Kvick, A.; Leiserowitz, L.; Nelson, M.; Weiner, S. Intercalation of sea-urchin proteins in calcite-study of a crystalline composite-material. *Science* **1990**, *250*, 664–667.

14. Berman, A.; Addadi, L.; Weiner, S. Interactions of sea-urchin skeleton macromolecules with growing calcite crystals—A study of intracrystalline proteins. *Nature* **1988**, *331*, 546–548.

15. Colfen, H. Bio-inspired mineralization using hydrophilic polymers. In *Biomineralization II: Mineralization Using Synthetic Polymers and Templates*; Springer-Verlag Berlin: Berlin, Germany, 2007; Volume 271, pp. 1–77.

16. Imai, H. Self-organized formation of hierarchical structures. In *Biomineralization I: Crystallization and Self-organization Process*; Springer: Berlin, Germay, 2007; Volume 270, pp. 43–72.

17. Song, R.Q.; Coelfen, H.; Xu, A.W.; Hartmann, J.; Antonietti, M. Polyelectrolyte-directed nanoparticle aggregation: Systematic morphogenesis of calcium carbonate by nonclassical crystallization. *ACS Nano* **2009**, *3*, 1966–1978.

18. Ye, G.; Nam, N.H.; Kumar, A.; Saleh, A.; Shenoy, D.B.; Amiji, M.M.; Lin, X.; Sun, G.; Parang, K. Synthesis and evaluation of tripodal peptide analogues for cellular delivery of phosphopeptides. *J. Med. Chem.* **2007**, *50*, 3604–3617.

19. Walton, A.G.; Blackwell, J. *Biopolymers*; Academic press: New York, NY, USA, 1973.

20. Deber, C.M. *Peptides: Structure and Function*; Pierce Chem. Co: Rockford, IL, USA, 1985.

21. Stahmann, M.A. *Polyamino Acids, Poly Peptides and Proteins*; University of Wisconsin Press: Wisconsin, WI, USA, 1962.

22. Block, H. *Poly(g-benzyl-l-glutamate) and Other Glutamicacid Containing Polymers*; Gordon and Breach: London, UK, 1983.

23. Kricheldorf, H.R. *A-amino Acid-N-Carboxyanhydrides and Related Heterocycles*; Springer Verlag: New York, NY, USA, 1987.

24. Kricheldorf, H.R. Polypeptides and 100 years of chemistry of alpha-amino acid n-carboxyanhydrides. *Angew. Chem. Int. Ed.* **2006**, *45*, 5752–5784.

25. Adams, D.J.; Young, I. Oligopeptide-based amide functional initiators for atrp. *J. Polym. Sci. A Polym. Chem.* **2008**, *46*, 6082–6090.

26. Aliferis, T.; Iatrou, H.; Hadjichristidis, N. Living polypeptides. *Biomacromolecules* **2004**, *5*, 1653–1656.

27. Deming, T.J. Facile synthesis of block copolypeptides of defined architecture. *Nature* **1997**, *390*, 386–389.

28. Deming, T.J. Amino acid derived nickelacycles: Intermediates in nickel-mediated polypeptide synthesis. *J. Am. Chem. Soc.* **1998**, *120*, 4240–4241.

29. Deming, T.J. Cobalt and iron initiators for the controlled polymerization of alpha-amino acid-*N*-carboxyanhydrides. *Macromolecules* **1999**, *32*, 4500–4502.

30. Dimitrov, I.; Schlaad, H. Synthesis of nearly monodisperse polystyrene-polypeptide block copolymers via polymerisation of *N*-carboxyanhydrides. *Chem. Commun.* **2003**, *23*, 2944–2945.

31. Kricheldorf, H.R.; Hauser, K. Polylactones. 55. A-B-A triblock copolymers of various polypeptides. Syntheses involving 4-aminobenzoyl-terminated poly(epsilon-caprolactone) as B block. *Biomacromolecules* **2001**, *2*, 1110–1115.

32. Yang, J.X.; Zhao, K.; Gong, Y.X.; Vologodskii, A.; Kallenbach, N.R. Alpha-helix nucleation constant in copolypeptides of alanine and ornithine or lysine. *J. Am. Chem. Soc.* **1998**, *120*, 10646–10652.

33. Lu, H.; Cheng, J. Hexamethyldisilazane-mediated controlled polymerization of alfa-amino acid *N*-carboxyanhydrides. *J. Am. Chem. Soc.* **2008**, *129*, 14114–14115.

34. Huang, J.; Habraken, G.; Audouin, F.; Heise, A. Hydrolytically stable bioactive synthetic glycopeptide homo- and copolymers by combination of NCA polymerization and click reaction. *Macromolecules* **2010**, *43*, 6050–6057.

35. Huang, J.; Bonduelle, C.; Thévenot, J.; Lecommandoux, S.; Heise, A. Biologically active polymersomes from amphiphilic glycopeptides. *J. Am. Chem. Soc.* **2012**, *134*, 119–122.

36. Vayaboury, W.; Giani, O.; Cottet, H.; Deratani, A.; Schue, F. Living polymerization of alpha-amino acid *N*-carboxyanhydrides (NCA) upon decreasing the reaction temperature. *Macromol. Rapid Commun.* **2004**, *25*, 1221–1224.

37. Deng, Z.; Habraken, G.J.M.; Peeters, M.; Heise, A.; de With, G.; Sommerdijk, N.A.J.M. Fluorescein functionalized random amino acid copolymers in the biomimetic synthesis of $CaCO_3$. *Soft Matter* **2011**, *7*, 9685–9694.

38. Davies, C.W. *Ion Association*; Butterworths: London, UK, 1962.

39. Corneille, F.; Copier, J.L.; Senet, J.P.; Robin, Y. Procédé de Préparation des *N*-carboxyanhydrides. Eur. Pat. Appl. 1201659, 2 May 2002.

40. Gibson, M.I.; Cameron, N.R. Experimentally facile controlled polymerization of *N*-carboxyan hydrides (NCAS), including O-benzyl-L-threonine NCA. *J. Polym. Sci. A Polym. Chem.* **2009**, *47*, 2882–2891.

41. Habraken, G.J.M.; Peeters, M.; Dietz, C.H.J.T.; Koning, C.E.; Heise, A. How controlled and versatile is *N*-carboxy anhydride (NCA) polymerization at 0 °C? Effect of temperature on homo-, block- and graft (co)polymerization. *Polym. Chem.* **2010**, *1*, 514–524.

42. Habraken, G.J.M.; Wilsens, K.H.R.M.; Koning, C.E.; Heise, A. Optimization of *N*-carboxyanhydride (NCA) polymerization by variation of reaction temperature and pressure. *Polym. Chem.* **2011**, *2*, 1322–1330.

43. Gebauer, D.; Voelkel, A.; Coelfen, H. Stable prenucleation calcium carbonate clusters. *Science* **2008**, *322*, 1819–1822.

44. Dandeu, A.; Humbert, B.; Carteret, C.; Muhr, H.; Plasari, E.; Bossoutrot, J.M. Raman spectroscopy—A powerful tool for the quantitative determination of the composition of polymorph mixtures: Application to $CaCO_3$ polymorph mixtures. *Chem. Eng. Technol.* **2006**, *29*, 221–225.

45. Lin, Y.P.; Singer, P.C. Inhibition of calcite crystal growth by polyphosphates. *Water Res.* **2005**, *39*, 4835–4843.

46. Sommerdijk, N.A.J.M.; de With, G. Biomimetic $CaCO_3$ mineralization using designer molecules and interfaces. *Chem. Rev.* **2008**, *108*, 4499–4550.

47. Malkaj, P.; Dalas, E. Calcium carbonate crystallization in the presence of aspartic acid. *Cryst. Growth Des.* **2004**, *4*, 721–723.

48. Manoli, F.; Dalas, E. Calcium carbonate crystallization in the presence of glutamic acid. *J. Cryst. Growth* **2001**, *222*, 293–297.

49. Cantaert, B.; Kim, Y.Y.; Ludwig, H.; Nudelman, F.; Sommerdijk, N.A.J.M.; Meldrum, F.C. Think positive: Phase separation enables a positively charged additive to induce dramatic changes in calcium carbonate morphology. *Adv. Funct. Mater.* **2012**, *22*, 907–915.

50. Evans, J.S. Tuning in to mollusk shell nacre- and prismatic-associated protein terminal sequences. Implications for biomineralization and the construction of high performance inorganic-organic composites. *Chem. Rev.* **2008**, *108*, 4455–4462.